JOURNAL OF CATALYSIS 89, 422–432 (1984)

The Interaction of Palladium with Alumina and Titanium Oxide Supports

R. T. K. BAKER, E. B. PRESTRIDGE,[1] AND G. B. MCVICKER

Corporate Research Science Laboratories, Exxon Research and Engineering Company, Clinton Township, Route 22 E, Annandale, New Jersey 08801

Received March 15, 1984; revised June 11, 1984

In a series of recent electron microscopy studies attempts were made to relate the phenomenological consequences of strong metal–support interactions (SMSI), such as suppressed chemisorption capacity, with morphological changes in either the support or supported metal particles. In the present investigation, a combination of high-resolution transmission electron microscopy and hydrogen chemisorption measurements were employed to address the sintering behavior of Pd supported on Al_2O_3 and TiO_2 following reduction at temperatures up to 800°C. Palladium was chosen, since it has the unique ability to both adsorb and absorb (β-hydride formation) hydrogen. This behavior was anticipated to provide an added dimension for characterizing SMSI systems. Palladium on alumina was selected as a control system. At reduction temperatures in excess of 700°C, Pd particles sinter on both Al_2O_3 and TiO_2 supports. The extent of sintering is, however, more extensive in the case of the TiO_2 support. The quantities of hydrogen adsorbed and absorbed by Pd/TiO_2 decreased in parallel with increasing reduction temperature, reaching essentially zero uptakes at reduction temperatures above 500–600°C. The amount of H_2 adsorbed by Pd/Al_2O_3 decreased about 60% upon increasing the reduction temperature from 500 to 700°C, in agreement with the extent of sintering detected by TEM which occurs within this temperature range. The quantity of H_2 absorbed by Pd/Al_2O_3, however, did not significantly decrease after reduction at 700°C. The anomalous behavior of Pd/TiO_2 is rationalized in terms of a model whereby reduction of TiO_2 to Ti_4O_7 leads to the simultaneous formation of mobile titanium suboxides, which are free to migrate onto the metal particle surface. The process ultimately results in the decoration of the Pd particles by titanium suboxide species. In this coated state, Pd is no longer capable of either adsorbing or absorbing hydrogen.

INTRODUCTION

In a series of electron microscopy investigations, we have attempted to relate the presence of strong metal–support interactions (SMSI state) with distinguishable morphological features of the metal particles (*1–4*). Studies of platinum on titanium oxide supported this view. When this system was heated in hydrogen at 550°C, the Pt crystallites took the form of thin, hexagonal-shaped "pillbox" structures and, contrary to other supports such as alumina, the metal crystallites did not increase in size when further heated to 800°C in hydrogen (*1*). Electron diffraction and lattice spacing measurements showed that, during reduction, the TiO_2 support transformed to Ti_4O_7, a change which was not detected in the absence of platinum.

The notion that characteristic particle morphologies or the inhibition of particle sintering could be used as a general diagnosis for the formation of a SMSI state was however dispelled during subsequent studies of nickel on titanium oxide (*4*). Electron microscopy examination showed that, at reduction temperatures of 700°C or higher, the Ni particles sintered. The larger Ni particles lost their well-defined faceted shapes becoming rounded and globular in appearance. Despite substantial sintering, other workers (*5, 6*) have reported that reduction above 450°C results in the suppression of the hydrogen chemisorption capacity of Ni/

[1] Analytical and Information Division, Exxon Research and Engineering Company, Clinton, New Jersey 08801.

0021-9517/84 $3.00

TiO_2. This feature has normally been associated with the attainment of the SMSI state (*7, 8*), however, recent work suggests that even this criterion may be suspect (*9*).

In the present investigation, we employed a combination of high-resolution transmission electron microscopy and hydrogen chemisorption measurements to address the sintering characteristics of palladium particles supported on alumina and titanium oxide, following reduction in hydrogen at temperatures up to 800°C. Palladium was selected as the metallic phase, as it has the property of both adsorbing and absorbing hydrogen (*10*). This characteristic was expected to provide an added dimension to the SMSI enigma. Thus, with palladium/titanium oxide, we could simultaneously determine the effect of the metal–support interaction on the formation of palladium hydride and on hydrogen chemisorption capacity. Palladium/alumina was selected as a control system, since it was anticipated that, on this support, palladium would exhibit normal hydrogen adsorption and absorption properties over a wide range of reduction temperatures.

Although there is continuing interest in the SMSI effect, it is surprising to find that the palladium/titanium oxide system is little studied. Vannice and co-workers (*11, 12*) examined the potential of this system as a CO hydrogenation catalyst and reported that it exhibited a higher turnover frequency for methanation than was found for palladium supported on silica, alumina, or silica–alumina. They rationalized these findings in terms of a model in which the higher methanation rates exhibited by palladium/titanium oxide result from relatively higher surface concentrations of hydrogen. The present studies were anticipated to provide further insight in the methanation model proposed by Vannice and coworkers.

EXPERIMENTAL

Electron Microscopy Studies

Transmission specimens of model catalysts were made by first sputtering thin films of titanium and aluminum oxide (35 nm thick) from the respective target materials onto rock salt crystals (2 × 2 cm). The rock salt was then dissolved in a water bath, leaving the oxide films floating on the surface. Pieces of these films were removed from the bath and thoroughly washed with water to remove traces of salt from their undersurfaces and finally mounted on stainless-steel electron microscope grids. Palladium was introduced simultaneously onto both sets of films by evaporation of spectrographically pure palladium wire from a heated tungsten filament at a residual pressure of 5×10^{-6} Torr. The amount of metal and distance of the source from the supported films was selected so that the deposited Pd film was about one monolayer thick.

These model catalyst specimens were then treated in a 20% hydrogen/helium mixture under flow conditions for 1 hr at 150, 500, 700, and 800°C—a fresh specimen being used for each temperature. After cooling, they were removed from the reactor and transferred in air to a Philips EM 300 transmission electron microscope. Particle size distributions were determined using a minimum of 500 particles at each temperature treatment.

Electron microscopy examinations were also performed on the conventionally prepared palladium/titanium oxide catalysts. In this case, the catalyst was ground to a fine powder and then ultrasonically dispersed in butyl alcohol. A drop of this suspension was applied to a holey carbon film mounted on a microscope grid. When these specimens were examined in the TEM, it was possible to find areas of the catalyst which were extremely thin (<25 nm) and which protruded from the carbon substrate. Particle size distributions were also determined for these specimens.

Preparation of Conventional Catalysts

A Degussa titanium oxide (60 m^2/g) was reduced under hydrogen (400 cm^3/min) at 800°C for 2.0 hr. Following reduction, the

sample was cooled to 600°C and then calcined under 20% oxygen/helium (500 cm^3/min) at this temperature for 1.0 hr. These treatments were used to sinter the titanium oxide support to a stable BET surface area of about 15–20 m^2/g (*13*).

Palladium catalysts (2 to 8 wt%) on γ-alumina (178 m^2/g) and presintered titanium oxide (20 m^2/g) supports were prepared by incipient wetness impregnation using aqueous HCl-acidified $PdCl_2$ solutions. The wet impregnates were dried at 120°C under dry air for 16 hr. The dried catalysts were analyzed for palladium content by the Analytical and Information Division, Exxon Research and Engineering Company, Linden, N.J.

Chemisorption Measurements

Hydrogen chemisorption measurements were performed with a conventional glass vacuum system employing a Texas Instruments fused quartz precision pressure gauge (*14, 15*). Prior to chemisorption measurements, the catalysts were reduced *in situ* under hydrogen (500 cm^3/min) for 2.0 hr at a temperature ranging between 175 and 700°C. A dual hydrogen adsorption–evacuation–readsorption isotherm procedure carried out at room temperature (near 22°C) was used to differentiate the quantity of hydrogen absorbed (β-hydride phase) and chemisorbed by the supported palladium particles (*16*).

X-Ray Measurements

X-Ray powder diffraction patterns were measured on a Philips Electronics Instruments diffractometer using nickel-filtered Cu($K\alpha$) radiation. Palladium metal and oxide crystallite sizes were estimated from the widths of the X-ray reflection lines, as described elsewhere (*17*).

RESULTS AND DISCUSSION

Electron Microscopy Studies

Palladium/titanium oxide. Examination of the micrographs obtained after reducing model palladium/titanium oxide samples in hydrogen over the temperature range 150 to 800°C (Figs. 1A–D), indicates that the particle morphologies exhibited by this system are substantially different from those shown by platinum/titanium oxide samples heated under the same conditions (*1*). At 500°C, even though the majority of Pd particles appear to be relatively thin, there is evidence that some particles are twinned, examples are circled in Fig. 1C. Such features suggest that these particular particles are greater than one-monolayer thick and are *not* flat structures (*18*). The incidence of twinning becomes more pronounced at 700°C, and the particles have undergone a significant increase in average size. Despite this size increase, the particles maintained a faceted outline. Following the 800°C reduction, it is apparent that particle growth continued, both laterally and in thickness. These larger crystallites tended to acquire a more globular morphology as edges and corners are rounded.

Inspection of the background of the four micrographs (Figs. 1A to D), shows that the appearance of the support also changes as the samples are heated from 150 to 800°C; this transformation commences at around 500°C. Electron diffraction examination reveals that a structural change from TiO_2 to Ti_4O_7 occurs during this temperature range. This support transition is the only feature which is consistently observed in metal/titanium oxide systems which exhibit SMSI behavior following high-temperature hydrogen reduction.

Particle size distribution (PSD) analyses of palladium/titanium oxide samples subjected to different reduction temperatures are presented in Fig. 2. From this data, it is evident that extensive sintering occurs at temperatures in excess of 500°C. Furthermore, comparison of the distributions obtained at 150 and 700°C shows that, although the average size of particles increase at the higher temperature, a significant fraction of particles actually become smaller. This behavior is consistent with

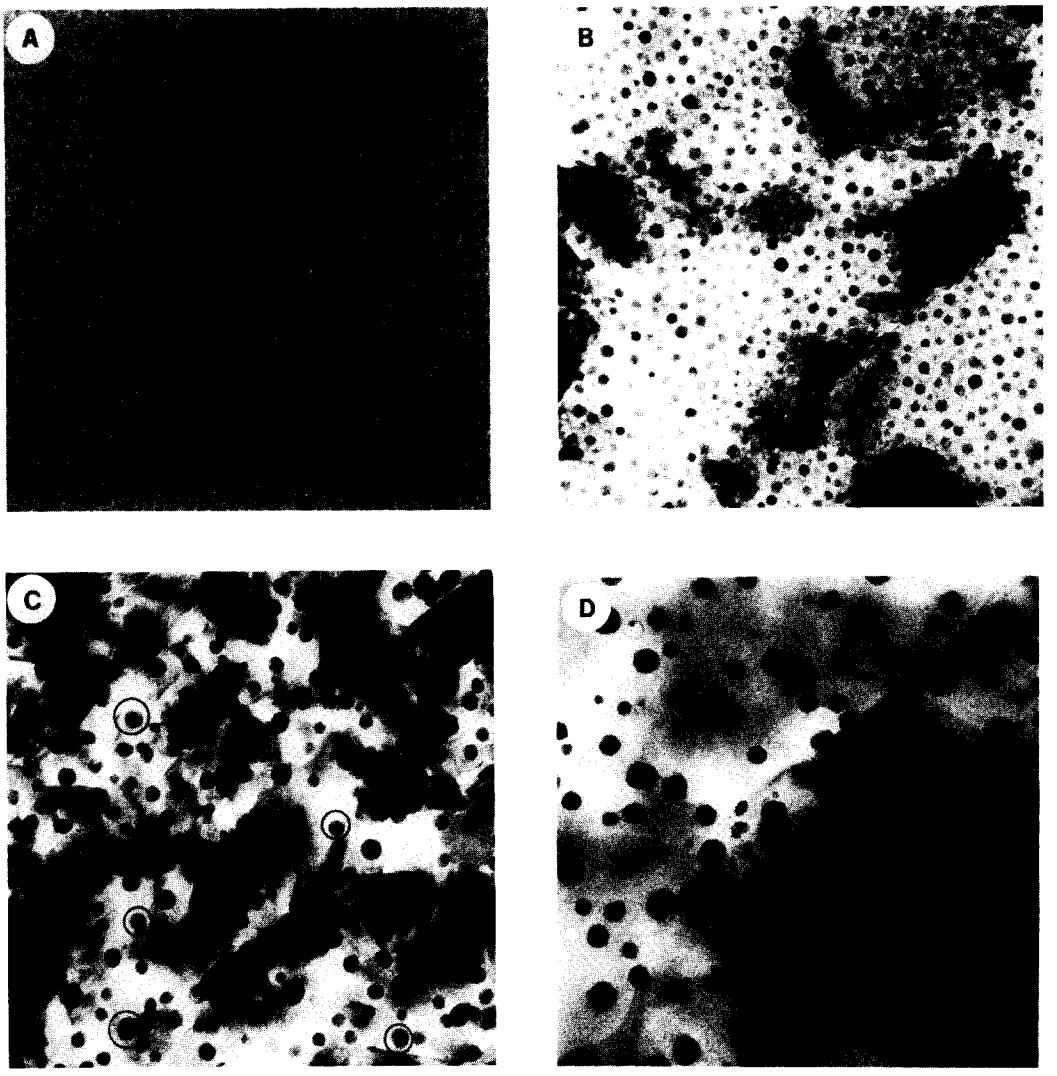

FIG. 1. (A–D) The appearance of palladium/titanium oxide specimens after reduction in hydrogen at 150, 500, 700, and 800°C, respectively.

the notion that sintering occurs by an atomic migration mode, a corollary of which is that large particles increase in size at the expense of smaller particles (*19a,b*).

A clearer appreciation of the differences in sintering behavior of palladium and platinum on titanium oxide can be obtained by comparing the average particle sizes of the two metals on TiO_2 as a function of reduction temperature (Fig. 3). Based on these and previous observations (*4*), the use of metal particle sintering inhibition as a criteria associated with the attainment of the SMSI state, does not appear to be universally valid.

Palladium/aluminum oxide. Figures 4A–D show the changes in appearance of palladium particles supported on aluminum oxide after reduction in hydrogen at the same conditions as those employed for treating palladium/titanium oxide samples. Although the particles increase in size by approximately a factor of two over the temperature range 500 to 800°C, there is no dramatic change in their morphological appearance. In general, the particles are of

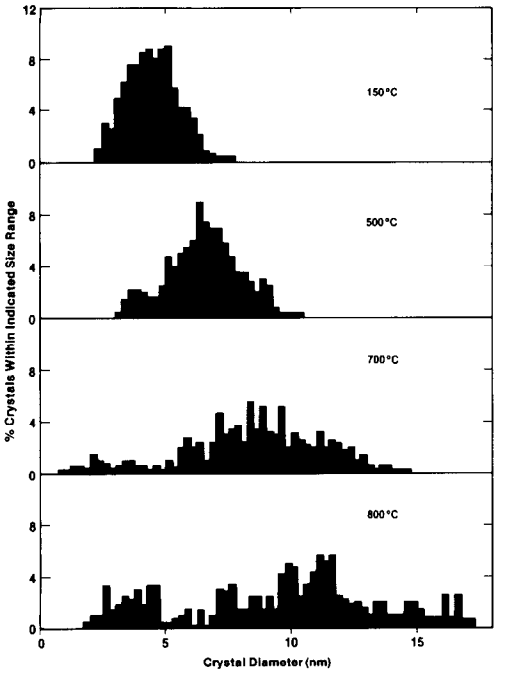

FIG. 2. Variation of PSD with reduction temperature for palladium on titanium oxide.

uniform density across their surface, and this aspect coupled with absence of twinned particles is indicative of a flat structure. Close inspection of the particle outlines reveal that their edges and corners tend to be rounded off. Furthermore, there is no evidence for "dumbbell" formation, which would be indicative of particle growth occurring by a crystallite migration mode (*20*). One must, therefore, conclude that sintering has occurred to the major extent via atomic migration. Chen and Ruckenstein have conducted a detailed investigation of Pd/Al_2O_3 and, according to them, the sintering mechanism is extremely complex (*21*).

In contrast to Pt/Al_2O_3 (*1, 22–24*), Pd/Al_2O_3 exhibits no sign of an interaction between the metal and the support at 800°C to form an alloy. Moreover, a more aggressive treatment, such as treatment in oxygen at 920°C, failed to destroy the discrete nature of the palladium particles (*25*).

Figure 5 shows the particle size distributions as a function of temperature and confirms the qualitative conclusions that the palladium/aluminum oxide system is relatively resistant toward sintering when treated in hydrogen.

Chemisorption Measurements

Typical room-temperature hydrogen isotherms, for 2 wt% palladium catalysts on γ-alumina and titanium oxide supports previ-

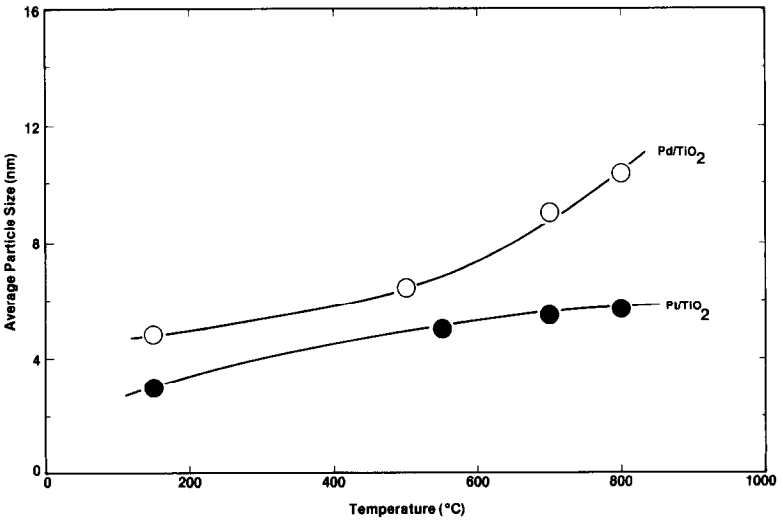

FIG. 3. Variation of mean metal particle size with reduction temperature for palladium and platinum on titanium oxide.

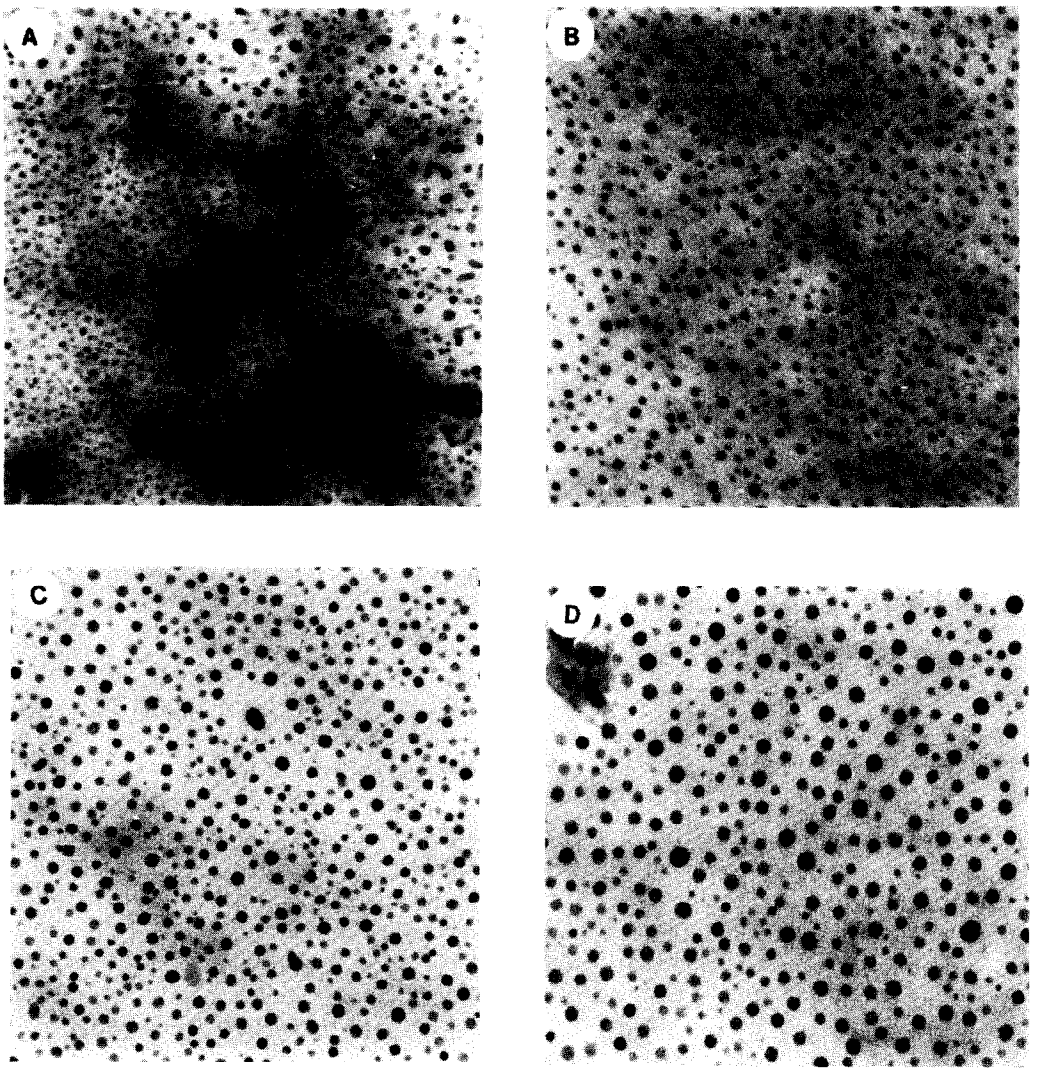

FIG. 4. (A–D) The appearance of palladium/aluminum oxide specimens after reduction in hydrogen at 150, 500, 700, and 800°C, respectively.

ously reduced at 350°C, are shown in Figs. 6 and 7, respectively. The quantities of hydrogen retained per gram of catalyst are expressed in terms of a gas volume corrected to standard conditions. From the zero-pressure intercept of the total hydrogen uptake curve, a H_T/Pd ratio is obtained (*26, 27*). Following the initial hydrogen uptake, the adsorption cell was evacuated ($\sim 10^{-6}$ Torr) at 22°C for 0.5 h, and a second isotherm was determined. The second isotherm provides a measure of the quantity of hydrogen absorbed by the supported palladium particles (*16*). A numerical value for H_{AB}/Pd is calculated from the zero-pressure intercept of the absorbed hydrogen curve. The difference between H_TPd and H_{AB}/Pd at zero pressure enables one to ascertain the number of hydrogen atoms irreversibly chemisorbed per palladium surface atom (H_S/Pd) at room temperature. For the 2% palladium/alumina catalyst reduced at 350°C, the H_T/Pd, H_{AB}/Pd, and H_S/Pd values are 0.91, 0.40, and 0.51, respectively (see Table

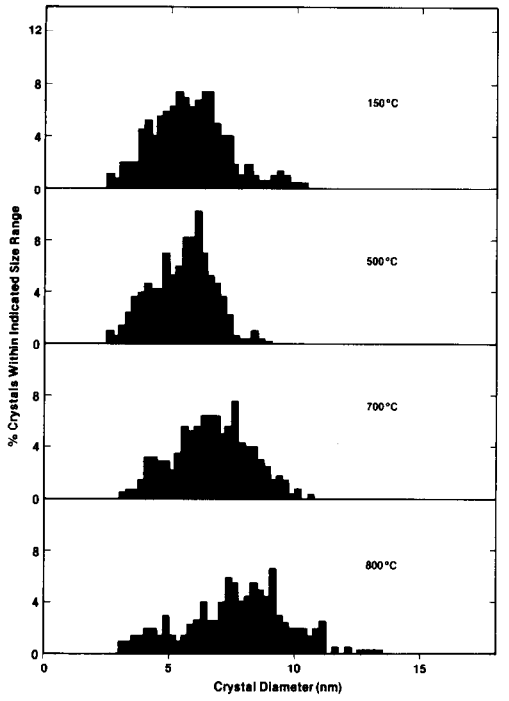

FIG. 5. Variation of PSD with reduction temperature for palladium on aluminum oxide.

1). The corresponding values for a 4% palladium/alumina catalyst reduced at 350°C are 0.78, 0.60 and 0.18, respectively. Using a similar adsorption–evacuation–readsorption procedure, Benson and co-workers (*16*) report H_TPd, H_{AB}/Pd, and H_S/Pd for a 5% palladium/alumina catalyst reduced at

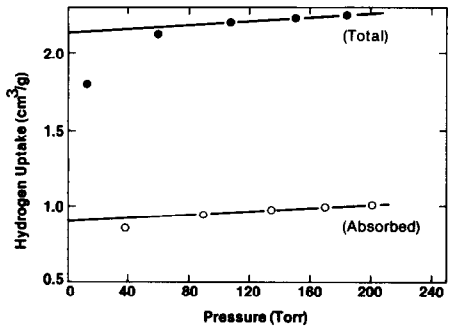

FIG. 6. Uptake of hydrogen on 2% Pd/Al_2O_3 at room temperature following 350°C reduction. Total isotherm is the initial isotherm, while the absorbed isotherm is a second isotherm determined after evacuation of the adsorption cell following the initial uptake to approximately 10^{-6} Torr for 0.5 hr at room temperature.

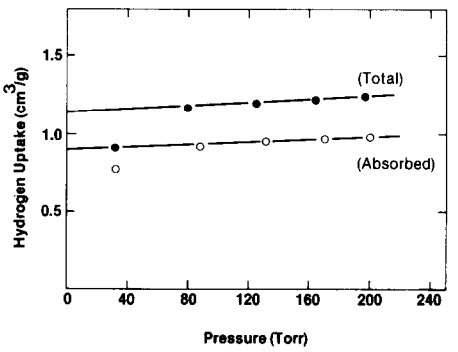

FIG. 7. Uptake of hydrogen on 2% Pd/TiO_2 at room temperature following 350°C reduction. Total isotherm is the initial isotherm, while the absorbed isotherm is a second isotherm determined after evacuation of the cell following the initial uptake to about 10^{-6} Torr for 0.5 hr at room temperature.

350°C of 0.71, 0.52, and 0.19, respectively. The lower H_S/Pd ratios shown by the 4 and 5% palladium catalysts, when compared to a 2% palladium/alumina, catalyst most likely reflects the decrease in dispersion expected at higher metal loadings (*28, 29*). By subtracting out the irreversible-bound hydrogen atom concentration, the apparent bulk hydride composition, H_{AB}/Pd_B, was calculated. The H_{AB}/Pd_B ratios for 2 and 4% palladium/alumina catalysts reduced at 350°C are 0.81 and 0.73, respectively. The 5% palladium/alumina catalyst studied by Benson and co-workers, by analogy, demonstrates an H_{AB}/Pd_B ratio of 0.64. In agreement with both the Benson and co-workers and the present studies, Vannice and co-workers (*12*) report an H_{AB}/Pd_B ratio of 0.74 for a 1.98% palladium/alumina catalyst. The calculated H_{AB}/Pd_B ratios for 2 and 4% palladium/alumina catalysts are somewhat higher than the 0.60 value expected for the β-hydride phase (*30*). This most likely results from a small amount of physically adsorbed hydrogen which overestimates the values of both H_T/Pd and H_{AB}/Pd by 10–20%.

Following reduction at 350°C, the 2% palladium/alumina catalyst exhibits an apparent H_S/Pd ratio, which is five times larger than the 2% palladium/titanium oxide cata-

TABLE 1

Effect of Reduction Temperature on the Uptake of Hydrogen by Palladium/Alumina and Palladium/Titanium Oxide Catalysts

Catalyst	Reduction conditions		Hydrogen/palladium ratios[a]			
	°C	t(hr)	H_T/Pd	H_{AB}/Pd	H_S/Pd	H_{AB}/Pd_B
2% Pd/Al_2O_3	175	2.0	0.97	0.47	0.50	0.94
	350	2.0	0.91	0.40	0.51	0.81
	500	2.0	0.79	0.40	0.39	0.66
	700	2.0	0.58	0.41	0.17	0.49
4% Pd/Al_2O_3	175	2.0	0.84	0.63	0.21	0.79
	350	2.0	0.78	0.60	0.18	0.73
	500	2.0	0.71	0.56	0.15	0.66
2% Pd/TiO_2	175	2.0	0.90	0.63	0.27	0.86
	350	2.0	0.53	0.43	0.10	0.48
	500	2.0	0.12	0.09	0.02	0.09
	700	2.0	0.05	0.05	0.00	—
	350	0.5	0.57	0.44	0.13	0.51
	350	1.5	0.53	0.43	0.10	0.48
	350	3.5	0.52	0.41	0.11	0.46
	350	7.5	0.49	0.39	0.10	0.43
	350[b]	0.5	0.59	0.47	0.12	0.53
4% Pd/TiO_2	175	2.0	0.74	0.60	0.14	0.70
	350	2.0	0.57	0.50	0.07	0.54
	500	2.0	0.16	0.15	0.01	0.15
8% Pd/TiO_2	175	2.0	0.70	0.64	0.06	0.68
	350	2.0	0.63	0.60	0.03	0.62
	500	2.0	0.38	0.38	0.00	—
	700	2.0	Nil	Nil	Nil	—

[a] The ratios H_T/Pd, H_{AB}/Pd, and H_S/Pd represent the total number of hydrogen atoms, the number of absorbed hydrogen atoms, and the number of surface chemisorbed hydrogen atoms per palladium atoms in the catalysts, respectively. The H_T/Pd and H_{AB}/Pd values were determined by extrapolation of the linear regions of the dual adsorption isotherms to zero pressure as illustrated in Figs. 5 and 6. The H_S/Pd values were determined by difference (H_T/Pd − H_{AB}/Pd) at zero pressure. H_{AB}/Pd_B represents the ratio of hydrogen absorbed to the number of bulk palladium atoms. This ratio was calculated by disregarding the surface-chemisorbed hydrogen atoms.

[b] Following a 7.5-hr reduction, the catalyst was calcined under oxygen for 2.0 hr at 350°C and then reduced under hydrogen at 350°C for 0.5 hr.

lyst (0.51 vs 0.10). Assuming a spherical crystallite geometry and a hydrogen atom to surface palladium atom adsorption stoichiometry of unity, these H_S/Pd values translate into average crystallite sizes of 2 and 12 nm, respectively, for the alumina- and titanium oxide-based catalysts. These crystallite sizes were calculated using the expression $D = 6 \times 10^4/S\rho$, where D is the diameter of the crystallite in Ångstroms, S is the metal surface area in m^2/g, and ρ is the density of palladium. The well-dispersed nature of the reduced 2% palladium/alumina catalyst was supported by complementary X-ray diffraction measurements which were devoid of palladium diffraction lines. In contrast, the 350°C-reduced 2% palladium/titanium oxide sample exhibited weak palladium lines, the widths of which indicated the presence of palladium particles 15–17 nm. Since the starting, unreduced 2% palladium/titanium oxide catalyst

did not show discernible palladium or palladium oxide lines—some sintering of particles occurred during reduction at 350°C. Measurements from electron micrographs of the sample reduced at 350°C showed that particles were in the size range, 1.1 to 11.2 nm, and the average size was about 4.0 nm. This latter value corresponds to an H_S/Pd ratio of 0.30, and so it is clear that the observed H_S/Pd ratio of 0.10 must be caused in part by processes other than sintering.

The effect of reduction temperature, on the uptake of hydrogen on a series of 2–8 wt% palladium catalysts on γ-alumina and titanium oxide supports, is summarized in Table 1. The H_T/Pd, H_{AB}/Pd, and H_S/Pd ratios for 2 and 4 wt% palladium on γ-alumina catalysts are fairly constant through a 175 to 500°C range of reduction temperatures. Reduction at 700°C, however, results in about a 50 to 60% decrease in the quantity of hydrogen chemisorbed on the surface palladium atoms and agrees with electron microscopy where Pd particles increased approximately twofold upon reducing at 700–800°C. Analogous observations have been reported by Aben (*31*) and were ascribed to palladium sintering at elevated reduction temperatures.

In contrast to palladium/alumina, 2 to 8 wt% palladium on titanium dioxide catalysts exhibited hydrogen uptakes which decreased continuously with increasing reduction temperature. Of particular interest is the systematic decrease in the H_{AB}/Pd and H_{AB}/Pd_B ratios with increasing reduction temperature and the absence of significant chemisorption (note the low H_S/Pd ratios) at temperatures above 500°C. TEM examinations clearly demonstrate that particle sintering increases as the temperature is raised (see Table 2). The inability of the larger palladium particles to absorb hydrogen (suppressed β-hydride formation) is totally unexpected. The absence of chemisorbed hydrogen following a high-temperature reduction, however, is consistent with the system being in the SMSI state.

The H_S/Pd ratio for 2% palladium/titanium oxide is lowered by a factor of about three upon increasing the reduction temperature from 175 to 350°C. It appears, therefore, that, even at the relatively low reduction temperature of 350°C, palladium on titanium oxide exhibits a pronounced SMSI effect. The partial SMSI effect observed at this temperature is not highly kinetically dependent, since the H_T/Pd, H_{AB}/Pd, and H_S/Pd ratios do not change over a reduction time interval from 0.5 to 7.5 hr. Following a 7.5-hr reduction, the 2% palladium/titanium oxide sample was calcined at 350°C under oxygen to disrupt the SMSI effect. Upon re-reduction at 350°C for 0.5 hr, the original hydrogen uptake values were reestablished. Thus, the extent of SMSI formation seems to depend primarily on reduction temperature and not on reduction time.

From a survey of the results presented here, some interesting additional features concerning the SMSI phenomenon emerge:

(a) Inhibition of particle growth and formation of a "pillbox" particle morphology are *not* necessary diagnostic properties of the SMSI state.

(b) Transformation of the support surface to a lower oxide state (e.g., $TiO_2 \rightarrow Ti_4O_7$ *does* appear to correlate with SMSI behavior).

TABLE 2

Effect of Reduction Temperature on the Average Particle Sizes of Palladium/Titanium Oxide Catalysts

Catalyst	Reduction conditions		Palladium particle diameters (nm)				
			XRD	H_S/Pd	TEM		
	°C	t (hr)			Min.	Ave.	Max.
2% Pd/TiO_2	175	2.0	NV[a]	4.3	1.0	3.3	7.5
	350	7.5	16	12	1.2	4.0	11.2
	500	2.0	14	58	—	—	—
	700	2.0	11	VL[b]	2.0	6.6	14.3
4% Pd/TiO_2	175	2.0	NV	8.3	1.2	3.2	8.1
	350	2.0	17	17	—	—	—
	500	2.0	16	116	1.5	4.6	15.5
8% Pd/TiO_2	175	2.0	NV	19	1.2	3.4	9.1
	350	2.0	18	39	—	0	—
	700	2.0	33	VL	2.1	6.8	23.4

[a] NV; not visible by X rays.

[b] VL; the absence of hydrogen chemisorption would indicate very large palladium particles.

(c) Finally, in the palladium/titanium oxide system, not only does the metal exhibit the expected decrease in hydrogen chemisorption capacity upon reduction at elevated temperatures, but also absorption of hydrogen is inhibited. This latter finding is extremely significant in view of the work of Boudart and Hwang (*32*), who found that the tendency of palladium on conventional supports to dissolve (absorb) hydrogen increased with increasing particle size.

We believe that all these features can be satisfactorily accounted for by the model proposed for the nickel–titanium oxide system (*4, 9*) and first suggested by Meriaudeau *et al.* (*33*) for platinum supported on titanium oxide. The key steps in this model are the reduction of TiO_2 to Ti_4O_7 with the simultaneous generation of mobile Ti or titanium oxide species, which are free to migrate onto the metal particle surfaces. This process initially leads to the decoration and eventually complete encapsulation of the metal particles. In this "buried" state, the metal particles are no longer able to either chemisorb or absorb hydrogen. In this context, it is worth recalling that Schuit and van Reijen (*34*) 25 years ago suggested the idea of "particle burying" to account for the loss of chemisorption capacity of nickel/silica catalysts following a reduction treatment. Finally, Cairns and co-workers (*35*) have used Nuclear Backscattering Spectrometry to demonstrate that interdiffusion can occur during high-temperature reduction (900–1000°C) of Pt and Rh on Al_2O_3 and TiO_2.

It is possible that the SMSI effect is in general a result of decoration and encapsulation; however, before coming to this conclusion, further studies specifically designed to probe the surfaces of the metal particles will be necessary.

REFERENCES

1. Baker, R. T. K., Prestridge, E. B., and Garten, R. L., *J. Catal.* **56,** 390 (1979).
2. Baker, R. T. K., Prestridge, E. B., and Garten, R. L., *J. Catal.* **59,** 293 (1979).
3. Baker, R. T. K., Prestridge, E. B., and Murrell, L. L., *J. Catal.* **79,** 348 (1983).
4. Simoens, A. J., Baker, R. T. K., Dwyer, D. J., Lund, C. R. F., and Madon, R. J., *J. Catal.* **86,** 359 (1984).
5. Mustard, D. G., and Bartholomew, C. H., *J. Catal.* **67,** 186 (1981).
6. Smith, J. S., Thrower, P. A., and Vannice, M. A., *J. Catal.* **68,** 270 (1981).
7. Tauster, S. J., Fung, S. C., and Garten, R. L., *J. Amer. Chem. Soc.* **100,** 170 (1978).
8. Tauster, S. J., and Fung, S. C., *J. Catal.* **55,** 29 (1978).
9. Jiang, X-Z., Hayden, T. F., and Dumesic, J. A., *J. Catal.* **83,** 168 (1983).
10. Axelrod, S. D., and Makrides, C. A., *J. Phys. Chem.* **68,** 2154 (1964).
11. Vannice, M. A., Wang, S-Y., and Moon, S. H., *J. Catal.* **71,** 152 (1981).
12. Wang, S-Y., Moon, S. H., and Vannice, M. A., *J. Catal.* **71,** 167 (1981).
13. Brunauer, S., Emmett, P. H., and Teller, E., *J. Amer. Chem. Soc.* **60,** 309 (1938).
14. Sinfelt, J. H., and Yates, D. J. C., *J. Catal.* **8,** 82 (1967).
15. McVicker, G. B., Baker, R. T. K., Garten, R. L., and Kugler, E. L., *J. Catal.* **30,** 146 (1973).
16. Benson, J. E., Hwang, H. S., and Boudart, M., *J. Catal.* **30,** 146 (1973).
17. Klug, H. P., and Alexander, L. E., *in* "X-Ray Diffraction Procedures for Polycrystalline and Amorphous Materials," 2nd ed., p. 687. Wiley, New York, 1974.
18. Marks, L. D., and Howie, A., *Nature (London)* **282,** 196 (1979).
19. (a) Flynn, P. L., and Wanke, S. E., *J. Catal.* **34,** 390 (1974); (b) McVicker, G. B., Garten, R. L., and Baker, R. T. K., *J. Catal.* **54,** 129 (1978).
20. Ruckenstein, E., and Pulvermacher, B., *AIChE J.* **19,** 356 (1973).
21. Chen, J. J., and Ruckenstein, E., *J. Catal.* **69,** 254 (1981).
22. Baker, R. T. K., Thomas, C., and Thomas, R. B., *J. Catal.* **38,** 510 (1975).
23. Sprys, J. W., and Mencik, Z., *J. Catal.* **40,** 290 (1975).
24. Dautzenberg, F. M., and Walters, H. B. M., *J. Catal.* **51,** 26 (1978).
25. Chen, J. J., and Ruckenstein, E., *J. Phys. Chem.* **85,** 1606 (1981).
26. Wilson, G. R., and Hall, W. K., *J. Catal.* **17,** 190 (1970).
27. Benson, J. E., and Boudart, M., *J. Catal.* **4,** 704 (1965).
28. Renouprez, A., Hoang-Van, C., and Compagnon, P. A., *J. Catal.* **34,** 411 (1974).
29. Yates, D. J. C., and Sinfelt, J. H., *J. Catal.* **8,** 348 (1967).

30. Lewis, F. A., "The Palladium Hydrogen System." Academic Press, New York/London, 1967.
31. Aben, P. C., *J. Catal.* **10,** 224 (1968).
32. Boudart, M., and Hwang, H. S., *J. Catal.* **39,** 44 (1975).
33. Meriaudeau, P., Dutel, J. F., Dufaux, M., and Naccache, C., *in* "Metal-Support and Metal-Additive Effects in Catalysis" (B. Imelik *et al.*, Eds.), Vol. 11, p. 95. Elsevier, Amsterdam, 1982.
34. Schuit, G. C. A., and van Reijen, L. L., "Advances in Catalysis," Vol. 10, p. 242. Academic Press, New York, 1958.
35. Cairns, J. A., Baglin, J. E. E., Clark, G. J., and Ziegler, J. F., *J. Catal.* **83,** 301 (1983).